Numerical modeling of magnetic induction and heating in injection molding tools

Guerrier, Patrick; Hattel, Jesper Henri

Published in:
Proceedings of International Conference on Advanced Manufacturing Engineering and Technologies (NEWTECH 2013)

Publication date:
2013

Numerical modeling of magnetic induction and heating in injection molding tools

Patrick Guerrier[1], Jesper H. Hattel[1]

[1]Technical University of Denmark, Department of Mechanical Engineering, Section of Manufacturing Engineering, Denmark
email pagu@mek.dtu.dk

ABSTRACT

Injection molding of parts with special requirements or features such as micro- or nanostructures on the surface, a good surface finish, or long and thin features results in the need of a specialized technique to ensure proper filling and acceptable cycle time. The aim of this study is to increase the temperatures as close as possible to the cavity surface, by means of an integrated induction heating system in the injection molding tool, to improve the fluidity of the polymer melt hereby ensuring that the polymer melt will continue to flow until the mold cavity is completely filled. The presented work uses numerical modeling of the induction heating in the mold to investigate how the temperature in the mold will be distributed and how it is affected by different material properties.

KEYWORDS: Induction heating, injection molding, finite element, coupled.

1. INRTRODUCTION

In order to injection mold special parts having micro- or nanostructures on the surface, being long and having thin features, or requiring a good surface finish, elevated mold temperatures will help ensuring complete filling of the cavity [1-3]. However, this can also lead to an increased cycle time due to a longer cooling time, if the heating is not only done locally where needed. The aim is therefore to only increase the temperature as close as possible to the surface by means of an induction heating system to improve the fluidity of the polymer melt hereby ensuring that the polymer melt will continue to flow until the mold cavity is completely filled. The temperature required will depend on the transition temperature of the polymer [1].

Recent studies [4-10] have been investigating induction heating of the mold tool, but they are mainly focused on using an induction coil to heat up the surface of the mold before the injection of the polymer. One drawback with this method is that a lot of the heat will already be dissipated out into the mold and away from the surface. This will in turn not be much warmer than without induction, as the whole mold will be heated up instead, again leading to a longer cooling time.

The basic idea behind this new concept is that a coil should be placed beneath the mold cavity surface, encased, on the backside, in a magnetic material, typically ferrite. The mold cavity in front should be made of a non-magnetic material electroplated with a layer of magnetic material e.g. nickel, to have the magnetic field running as close as possible to the surface of the cavity side.

The presented work uses numerical modeling of the induction heating in the mold to investigate the temperature distribution in the mold and especially at its surface. There are two main mechanisms taking place in induction heating, namely electromagnetism and thermal conduction. The electromagnetism is described by Maxwell's equations which need to be solved. A rapid changing magnetic field induces Eddy currents, which gives rise to a resistive heating effect, known as Joule heating. The thermal conduction is controlled by the heat conduction equation wherein the Joule heating is acting as a source term. The Eddy currents tend to run at the surface of a magnetic conducting material due to the well-known effect of the skin depth [11]. It is desired to find a combination of materials with different electrical properties to get the heating as close as possible to the cavity surface. In this study different material properties are investigated to find such a combination.

2. MECHANISMS

The electromagnetic part of induction heating is controlled by Maxwell's equations, which here are presented in terms of free charges and currents [12]:

$$\nabla \cdot \mathbf{D} = \rho_f \tag{1}$$

$$\nabla \cdot \mathbf{B} = 0 \tag{2}$$

$$\nabla \times \mathbf{E} = -\frac{\partial \mathbf{B}}{\partial t} \tag{3}$$

$$\nabla \times \mathbf{H} = \mathbf{J}_f + \frac{\partial \mathbf{D}}{\partial t} \tag{4}$$

Where $\mathbf{D}$ is the electric flux density, $\mathbf{B}$ is the magnetic flux density, $\mathbf{E}$ is the electric field, $\mathbf{H}$ is the magnetic field, $\mathbf{J}_f$ is the free current density, ρ_f is the free charge density, t is the time. Relating $\mathbf{D}$ and $\mathbf{H}$ in terms of $\mathbf{E}$ and $\mathbf{B}$ depends on the material, and for linear media it can be related through the following constitutive relations:

$$\mathbf{D} = \varepsilon \mathbf{E} = \varepsilon_0 \varepsilon_r \mathbf{E} \tag{5}$$

$$\mathbf{H} = \frac{1}{\mu}\mathbf{B} = \frac{1}{\mu_0 \mu_r}\mathbf{B} \tag{6}$$

Where ε_0 is the vacuum permittivity, ε_r is the relative permittivity, μ_0 is the vacuum permeability, and μ_r is the relative permeability. Furthermore the current density and electric field can be related by the well-known Ohm's law:

$$\mathbf{J} = \sigma \mathbf{E} \tag{7}$$

Where σ is the electrical conductivity. The displacement current in equation (4) will be ignored and the assumption that a time-harmonic varying source current density will result in a sinusoidally varying magnetic field will be made. Combining Maxwell's equations (1)-(4) with the constitutive equations (5)-(7), the following complex diffusion equation can be derived [11]:

$$\frac{1}{\mu}\nabla^2\overline{\mathbf{A}} - i\omega\sigma\overline{\mathbf{A}} = -\overline{\mathbf{J}}_s \tag{8}$$

Where $\overline{\mathbf{A}}$ is the magnetic vector potential related to the magnetic flux by $\mathbf{B} = \nabla \times \mathbf{A}$, $\overline{\mathbf{J}}_s$ is the source current density in the coil, $\omega = 2\pi f$ is the angular frequency (and f the frequency), and the overbar is denoting the peak value or the amplitude. Assuming an axisymmetric cylindrical system, the magnetic vector potential has an azimuthal component only and equation (8) reduces to:

$$\frac{1}{\mu}\left(\frac{1}{r}\frac{\partial}{\partial r}\left(r\frac{\partial \overline{A}_\theta}{\partial r}\right) + \frac{\partial^2 \overline{A}_\theta}{\partial z^2}\right) - i\omega\sigma\overline{A}_\theta = -\overline{J}_{s,\theta} \tag{9}$$

The magnetic flux can be found from the solution of the magnetic vector potential by taking the curl of $\overline{A}_\theta$, hence for the axisymmetric case it can be calculated as:

$$\overline{B}_r = -\frac{\partial \overline{A}_\theta}{\partial z}; \quad \overline{B}_z = \frac{\partial \overline{A}_\theta}{\partial r} + \frac{\overline{A}_\theta}{r} \tag{10}$$

The magnetic field can then be found using equation (6). The induced Eddy currents in the conductors can be found from:

$$\overline{J}_e = -i\omega\sigma\overline{A}_\theta \tag{11}$$

From which the Joule heating can be found via:

$$\dot{Q} = \frac{1}{2\sigma}\left|\overline{J}_e\right|^2 \tag{12}$$

Which is the volumetric heat source induced by the Eddy currents. A well-known and useful expression is the current skin depth or penetration depth, which can also be derived from Maxwell's equations. This quantity is defined as the distance for which the amplitude of a plane wave decreases by a factor of $e^{-1} = 0.368$, and will prove useful later:

$$\delta = \frac{1}{\sqrt{\pi f \mu \sigma}} \tag{13}$$

The other mechanism taking place in induction heating is the heat conduction, which can be described by the transient heat conduction equation:

$$\rho c_p \frac{\partial T}{\partial t} = k\nabla^2 T + \dot{Q} \tag{14}$$

Where T is the temperature, ρ is the density, c_p is the specific heat capacity, k is the thermal conductivity, and $\dot{Q}$ is the heat source from equation (12).

3. FINITE ELEMENT FORMULATION

The finite element method has been used to solve equation (9) and (14). This implies first finding the heat source term from the electromagnetic solution and then using it in the transient heat conduction equation to get the resulting temperature distribution. The implementation of the finite element formulation is done in-house and is self-developed using MATLAB. The implementation is tested against the commercial software COMSOL and QuickField, to validate the code. For the actual experimental setup presented here, it was chosen to use the self-developed implementation due to its code flexibility and fast solution time. Using the Galerkin method to approximate the solution on a set of discrete points we get

$$\int_\Omega [N]^T \left[\frac{1}{\mu}\left(\frac{1}{r}\frac{\partial}{\partial r}\left(r\frac{\partial \bar{A}_\theta}{\partial r}\right) + \frac{\partial^2 \bar{A}_\theta}{\partial z^2}\right) - i\omega\sigma\bar{A}_\theta + \bar{J}_{s,\theta}\right] d\Omega = 0 \tag{15}$$

where $[N]$ is a row vector containing the shape functions, and Ω is the domain of interest. The total matrix system becomes:

$$[[K] + i[C]]\{\bar{A}_\theta\} = \{f\} \tag{16}$$

with the following element matrix equations:

$$[K]_e = \int_\Omega \frac{1}{\mu}[B]^T[B]d\Omega\,; \quad [C]_e = \int_\Omega \omega\sigma[N]^T[N]d\Omega\,; \quad \{f\}_e = \int_\Omega \bar{J}_s[N]^T d\Omega \tag{17}$$

where $[B]$ is the derivative of the shape function also called gradient matrix. Linear triangular elements have been employed and a closed form solution of the integration has been done with the resulting elemental matrices being similar to those described in [11].

The heat conduction equation is discretized in a similar way. Employing equation (14) in cylindrical coordinates and using the Galerkin method we obtain

$$\int_\Omega [N]^T \left[k\left(\frac{1}{r}\frac{\partial}{\partial r}\left(r\frac{\partial T}{\partial r}\right) + \frac{\partial^2 T}{\partial z^2}\right) + \dot{Q} - \rho c_p \frac{\partial T}{\partial t}\right] d\Omega = 0 \tag{18}$$

Inserting the spatial approximation of the temperature will then result in the following form of matrix equation:

$$[C]\left\{\frac{\partial T}{\partial t}\right\}+[K]\{T\}=\{f\} \tag{19}$$

With similar element matrices to those in equation (17) but substituting $\frac{1}{\mu}$ with k, $\omega\sigma$ with ρc_p, and $\bar{J}_s$ with $\dot{Q}$. The time derivative is discretized using an implicit Euler approximation (backward finite difference) to yield the following form:

$$([C]+\Delta t[K])\{T\}^{n+1}=[C]\{T\}^{n}+\Delta t\{f\} \tag{20}$$

Where Δt is the time step. The implicit formulation has the advantage of being unconditionally stable. Both equation systems seen in equation (16) and (20) are built as sparse matrices and both are solved using MATLAB's build-in solver, which can solve unsymmetrical sparse linear systems on the form $[A]\{x\}=\{b\}$.

4. GEOMETRICAL SETUP

An induction heating setup has been employed with the self-developed finite element code and in COMSOL. Only the results from the self-developed code will be shown as they are identical to the COMSOL implementation. This is done to investigate the temperature distribution in the mold utilizing a unique combination of materials to get the Eddy currents as close as possible to the mold cavity. All components have been integrated into the mold itself, in order to avoid external inductors to heat the mold surface. Also, the unit can be used with a conventional injection molding machine, with the only extra equipment being the power supply.

The mold seen in Fig. 1 consists of a mold plate, which from the backside contains a core with a coil inserted. The coil consists of windings of insulated copper wires. The core (or field concentrator) is used to carry the magnetic flux and to concentrate it where it is needed, here in front of it towards the surface of the mold plate.

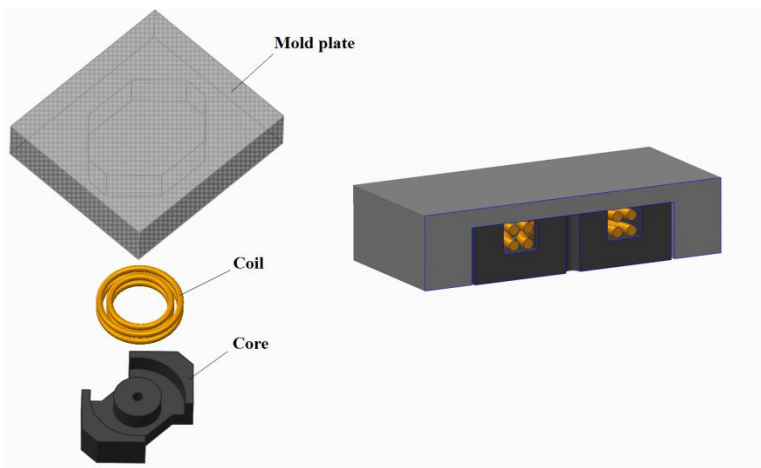

Fig.1. Left: Exploded view of the main parts in the mold with the build-in inductor. Right: Cross section of the mold with the cavity side up, where the molten polymer will flow.

5. NUMERICAL MODEL SETUP

In the finite element model it is assumed that the geometry is axisymmetric, and consists of a cross section as seen in both Fig. 1 to the right and in Fig. 2. Besides the mold plate, core, and coil other features in the geometry includes an added layer of a magnetic material on the top of the mold plate. The magnetic layer's purpose is to carry the magnetic field as close as possible to the cavity surface. The coil is encased in a non-conducting material like a polymer, and inside each winding is a cooling channel, which prevents the coil from being heated up due to Joule heating.

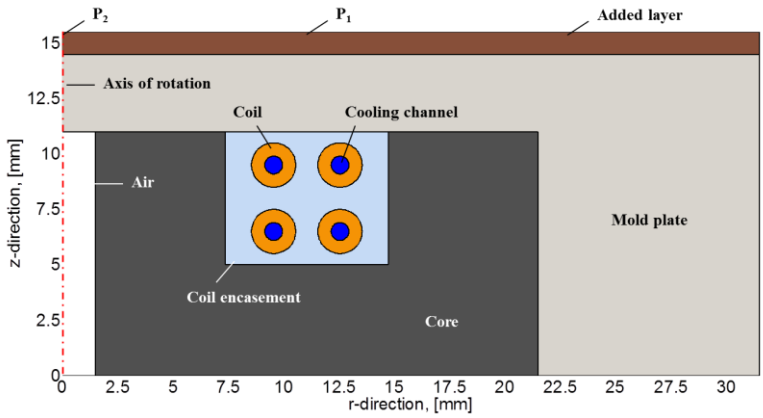

Fig.2. Detailed drawing of the sections in the axisymmetric numerical model

The boundaries in the models are of Dirichlet type at the axis of symmetry for the electromagnetic field, as the field vanishes toward the symmetry axis. The same type of boundary is also used for the three other outer boundaries, as the field also vanishes towards those, due to the magnetic material carrying the magnetic flux.

The current density is applied in the coils, and it is assumed that each winding carries 200 A at a frequency of 10 kHz. This gives a current density of approximately $7.6 \cdot 10^7$ A/m^2.

The boundaries for the heat conduction equation are adiabatic (neutral Neumann condition) at all the outer boundaries. For all material interfaces the heat transfer coefficient is set to infinity. The cooling channel domains are set to a Dirichlet type condition with a specified temperature of the cooling channel liquid. This is chosen to be the initial temperature of the mold which is room temperature at 25°C. The time step used in the simulation was 0.1 seconds. The electrical and thermal material data used for the finite element calculation have been summarized in Table 1.

A two-step coupling between the electromagnetic and thermal solution is used. This has been chosen because the material data are assumed to be constant, and not depend on temperature. This approximation can give good results at low temperatures (<200°C) [11] and is very efficient to employ, as the complex steady state diffusion equation (9) only needs to be solve once to find the heat source term, which can then be switched on and off as desired in the transient thermal analysis.

Table 1. Electromagnetic and thermal properties used for the different materials (sections)

Material	**Relative permea-Bility [-]**	**Electrical conductivity [S/m]**	**Thermal conductivity [W/mK]**	**Density [kg/m^3]**	**Specific heat capacity [J/kgK]**
Air	1	0	0.0257	1.205	1.005
Copper (Coil)	1	6e7	400	8700	385
Ferromagnetic ceramic (Core)	600	100	4	5000	700
Non-magnetic Steel (Mold)	1	1.45e6	28	7750	460
Nickel (Layer)	100	1.43e7	91	8900	460
Silicone (Enca.)	1	3.16e-12	0.3	1550	1200

Due to the skin depth the current will run in a thin layer in the magnetic materials. This gives a rather strict requirement for the mesh in the magnetic layer in order to get sufficiently accurate results. A good practice [11] is to have at least three skin depths of fine mesh. At three skin depths the current is reduced to $e^{-3} = 0.05$ of its original value, meaning that 95% of the currents will run in the fine mesh. For the mold plate the skin depth can be calculated to be $\delta = 4.18$ mm and for the magnetic layer to be $\delta = 0.1336$ mm, so a maximum element size of 0.315 mm should satisfy the requirement in the mold and 0.0550 mm in the nickel layer at the boundary facing the mold plate should satisfy the requirement in the magnetic layer. The mesh, see Fig. 3, has been created in COMSOL and subsequently imported into the in-house developed FE-code.

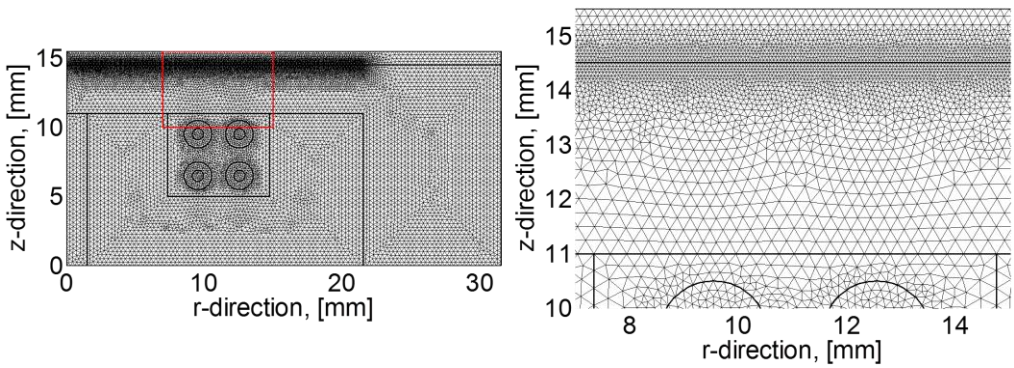

Fig.3. Left: The mesh used in the numerical model with 29.013 elements and 14.698 nodes. Right: Close up look at the mesh above the inductor, where a substantial amount of elements is required due to the skin depth.

6. RESULTS AND DISCUSSION

The solution time of the MATLAB implementation is around 11 seconds, compared to the COMSOL validation simulation (linear elements and 1st order accuracy in time) which takes around 15 seconds. From the solution of equation (9) the magnetic flux is found, and the flux lines are depicted in Fig. 4. It can be seen that the magnetic field is concentrated in front of the core, and the flux lines move relatively easy through the mold material and into the magnetic layer which carries the flux in a very thin layer due to the skin depth.

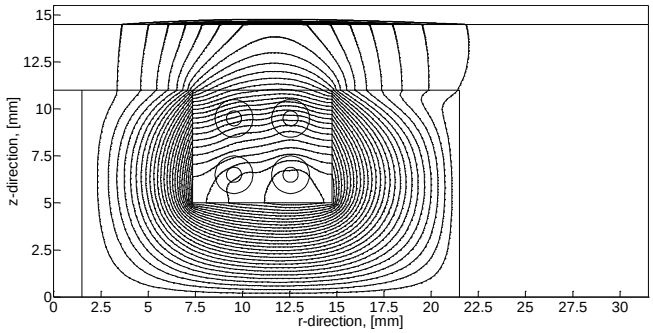

Fig.4. Contours of equal magnetic vector potential magnitudes or the magnetic flux lines induced by the coil.

Figure 5 shows the Joule heat arising from the Eddy currents, which are found directly from the electromagnetic solution using equation (11) and (12). In the figure to the left it is possible to see the distribution in the z-direction. A high peak is observed in the layer, but also a lot of heat is generated in the mold plate itself.

The reason for the substantial amount of heat generated in the mold, even though it is a non-magnetic material, can be related back to the skin depth, equation (13), as both the electrical conductivity and the permeability contribute to how deep the currents run in a material. This means that lowering the electrical conductivity further in the mold material will allow the magnetic flux to easier penetrate the mold, and be concentrated in the magnetic layer close to the cavity. A ten times lower electrical conductivity in the mold will give a skin depth of δ = 13.22 mm compared to 4.18 mm, which is an indication that the magnetic flux can more easily penetrate the mold and into the magnetic layer.

Different variations of the electrical conductivity have been tested for the mold material and for the magnetic layer. In Fig. 6 the Joule heating in the z-direction can be seen using different combinations of electrical conductivity. The red curve to the left is the same curve as in Fig. 5 to indicate the difference in magnitude.

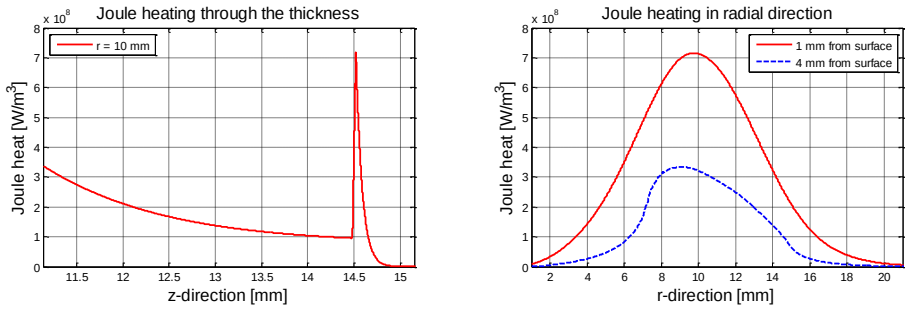

Fig.5. Joule heat distribution in different positions: Left: in the z-direction above the inductor (here, a high peak is observed in the magnetic layer). Right: in the radial direction at different distances from the mold cavity surface.

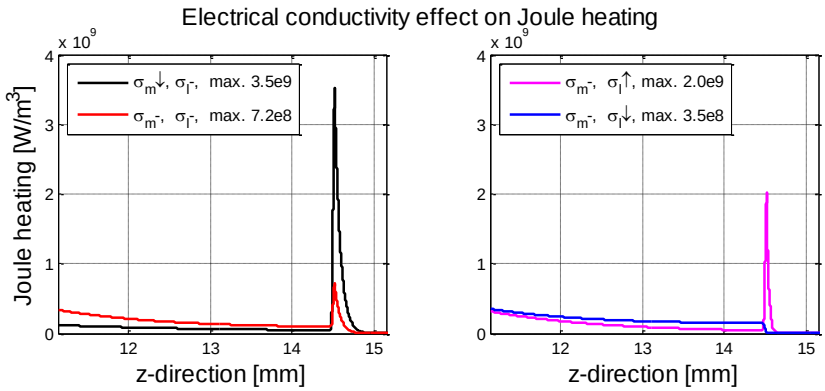

Fig.6. Distribution of the Joule heat in the z-direction above the inductor for different electrical conductivities, σ, in the mold (denoted with m) and the layer (denoted with l). Downward pointing arrow means a ten times lower conductivity, and upward pointing arrow means a ten times higher. Having a low electrical conductivity in the mold is favorable.

A clear improvement can be seen for a (here ten times) lower electrical conductivity in the mold material. Raising the electrical conductivity of the magnetic layer does give a higher Joule heating in the layer. It still generates a lot of heat in the mold plate which is not favorable, and gives an even stricter requirement for the mesh. What is the most interesting is how lowering the electrical conductivity of the mold plate will promote the Joule heating in the magnetic layer, resulting in an effect which is greatly desirable for this setup. The temperature distribution in the mold can been seen in Fig. 7 after four seconds of heating for both standard and low value of the electrical conductivity of the mold plate.

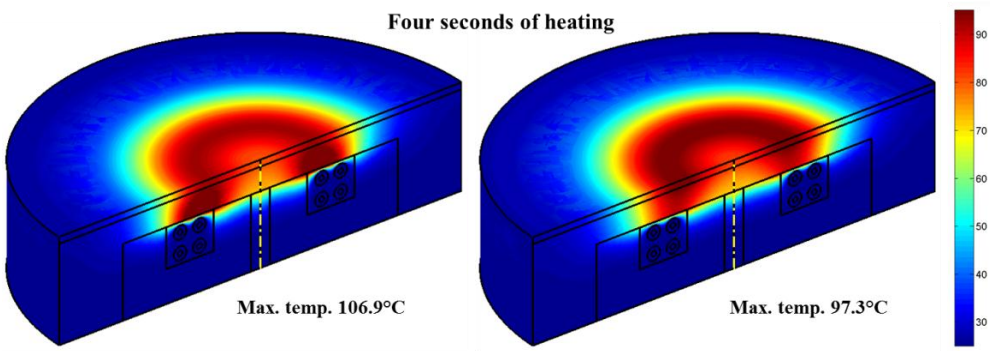

Fig.7. Left: (Unfavorable) Temperature distribution after four seconds of induction heating using the electrical conductivities specified in Table 1. Right: (Favorable) Temperature distribution after four seconds of induction heating using a ten times lower electrical conductivity in the mold as compared to Table 1.

Even though the maximum temperature after four seconds is higher for the simulation with standard electrical conductivity in the mold plate, it is located close to the inductor and not at the surface where it is desired. This means a higher amount of energy would have to be removed after the injection phase, making it more energy inefficient. The transient behavior of the temperature at two measurement points P_1 (surface) and P_2 (center: Axis-symmetric line at the surface) shown in Fig. 2 and the maximum temperature at any given point are shown in Fig. 8 for four seconds of induction heating and four seconds of cooling.

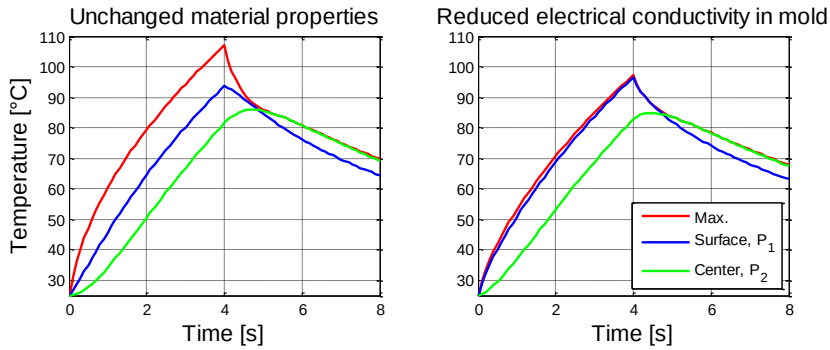

Fig.8. Comparison of the temperature at the surface above the inductor (P_1), center of the mold (P_2), and the maximum temperature, during four seconds of heating and four seconds of cooling, without (left) (unfavorable) and with (right) (favorable) a ten time reduction in the electrical conductivity of the mold.

It is evident that the temperature at the surface above the inductor is very close to the maximum temperature during the heating phase, and still cools down together with the center point, when having a low electrical conductivity in the mold. It should be noted that the simulations were done with the mold being at room temperature initially, so the cooling phase of both simulations in Fig. 8 are quite similar, but it is expected that having a lower electrical conductivity in the mold will reduce the cooling phase when a steady cycle is reached.

7. CONCLUSION

A finite element model of an induction heating system to be used in an injection mold has been presented. The main mechanisms and their associated equations, namely the complex steady state diffusion equation and the transient heat conduction equation, have been presented. The finite element discretization using the Galerkin method is also presented. The model is subsequently used in a study of an injection molding tool with a built-in inductor, where the Joule heating and temperature distribution were investigated. An interesting finding was, that using a magnetic layer on the cavity surface alone is not enough to promote a maximum temperature field in the surface. Due to the skin depth, a non-magnetic material with a low electrical conductivity will be needed in order to promote the heating of the tool as close as possible to the cavity surface.

REFERENCES

[1] K. Crow and R. Foad, "Is Rapid Temperature Cycling the Long Awaited Panacea for Injection Molded Parts," *Soc. of Plastics Eng.*, pp. 1544-1550, 2012.

[2] Y. Shen and W. Wu, "An analysis of the three-dimensional micro-injection molding," *Int. Commun. Heat Mass Transfer*, vol. 29, pp. 423-431, 2002.

[3] Y. K. Shen et al., "Three-dimensional non-Newtonian computations of micro-injection molding with the finite element method," *Int. Commun. Heat Mass Transfer*, vol. 20, pp. 643-652, 2002.

[4] S. C. Chen et al., "Simulations and verifications of induction heating on a mold plate," *Int. Comm. Heat Mass Transfer*, vol. 7, pp. 971-980, 2004.

[5] H. Eom and K. Park, "Fully-Coupled Numerical Analysis of High-Frequency Induction Heating for Thin-Wall Injection Molding," *Polymer-Plastics Tech. and Eng.*, vol. 48, pp. 1070-1077, 2009.

[6] H. Eom and K. Park, "Integrated Numerical Analysis to Evaluate Replication Characteristics of Micro Channels in a Locally Heated Mold by Selective Induction," *Int. J. Of Precision Eng. And Manufacturing*, vol. 12, pp. 53-60, 2011.

[7] M.-S. Huang et al., "Electromagnetic Induction Coil Design for Mold Surface," *Soc. of Plastics Eng.*, pp. 1471-1476, 2012.

[8] H.-L. Lin et al., "Induction heating with the ring effect for injection molding plates," *Int. Commun. in Heat and Mass Transfer*, vol. 39, pp. 514-522, 2012.

[9] K. Park and S.-I. Lee, "Localized mold heating with the aid of selective induction for injection molding of high aspect ratio micro-features," *J. Of Micromechanics And Microengineering*, vol. 20, pp. 1-11, 2010.

[10] Y.-T. Sung et al., "Design of Induction Heating Module for Uniform Cavity," *Soc. of Plastics Eng.*, pp. 1427-1436, 2012.

[11] V. Rudnec et al., Handbook of Induction Heating, Marcel Dekker, Inc., 2003.

[12] D. J. Griffiths, Introduction to Electrodynamics, Prentice Hall, 1999.